European Journal of Neuroscience, Vol. 17, pp. 1811–1819, 2003

Rhythm sequence through the olfactory bulb layers during the time window of a respiratory cycle

Nathalie Buonviso, Corine Amat, Philippe Litaudon, Stephane Roux,[1] Jean-Pierre Royet, Vincent Farget and Gilles Sicard

Neurosciences et Systèmes Sensoriels, Université Lyon I CNRS, 50 avenue Tony Garnier, 69366 Lyon cedex 07, France
[1]Laboratoire de Physique, ENS-Lyon, 46, allée d'Italie, 69364 Lyon cedex 07, France

Keywords: LFP, olfactory bulb, oscillations, rat, synchronization

Abstract

The mammalian olfactory bulb is characterized by prominent oscillatory activity of its local field potentials. Breathing imposes the most important rhythm. Other rhythms have been described in the β- and γ-frequency ranges. We recorded unitary activities in different bulbar layers simultaneously with local field potentials in order to examine the different relationships existing between (i) breathing and field potential oscillations, and (ii) breathing and spiking activity of different cell types. We show that, whatever the layer, odour-induced γ oscillations always occur around the transition point between inhalation and exhalation while β oscillations appear during early exhalation and may extend up to the end of inhalation. By contrast, unitary activities exhibit different characteristics according to the layer. They vary in (i) their temporal relationship with respect to the respiratory cycle; (ii) their spike rates; (iii) their temporal patterns defined according to the respiratory cycle. The time window of a respiratory cycle might thus be split into three main epochs based on the deceleration of field potential rhythms (from γ to β oscillations) and a simultaneous gradient of spike discharge frequencies ranging from 180 to 30 Hz. We discuss the possibility that each rhythm could serve different functions as priming, gating or tuning for the bulbar network.

Introduction

Slow (1–8 Hz) high amplitude waves are a prominent characteristic of the electrophysiological activity of the olfactory system, particularly during odour sampling. These field potential waves are related to respiration and have been observed in the olfactory bulb (OB) as well as in the piriform cortex (Adrian, 1950; Freeman & Schneider, 1982; Bressler, 1987). Such a respiratory modulation has also been described in the OB mitral/tufted cell unitary activities (Walsh, 1956; Macrides & Chorover, 1972; Chaput & Holley, 1980; Onoda & Mori, 1980; Mair, 1982; Pager, 1985; Chaput, 1986). Rather than a variation in overall firing frequency, odour-evoked mitral/tufted cell responses have often been reported as a temporal reorganization of its discharge into inhalation-related bursts of spikes.

Coexisting with this slow modulation, rhythmic activities in higher frequency bands are present in the mammalian OB field potentials. Gamma band (40–80 Hz) oscillatory activity, first observed by Adrian (1950) in the hedgehog, was intensively investigated by Freeman and coworkers (for review, see Freeman, 1975). These oscillations have been interpreted as the action of local inhibitory circuits in the granule–mitral cell loop (Rall & Shepherd, 1968). It has been proposed that they play a key role in encoding olfactory representations (Freeman, 1975; Laurent & Davidowitz, 1994). Beta-frequency (15–35 Hz) activity was also observed in the OB (Heale & Vanderwolf, 1994; Chapman *et al*., 1998; Kay & Freeman, 1998). Its origin is less clear, believed to be cortical for some investigators (Bressler, 1987) and bulbar for others (Chapman *et al*., 1998; Kay & Freeman, 1998). Very few studies in the mammal examined γ or β band oscillations at the single-unit level. Desmaisons *et al*. (1999) showed in OB slices that mitral cells display spontaneous subthreshold oscillations of their membrane potential, ranging from 10 to 50 Hz as a function of resting membrane potential level. Using extracellular recordings, Kashiwadani *et al*. (1999) showed that the odour-evoked spike discharge of mitral/tufted cells tended to phase-lock to the oscillatory field potential in the ≈37-Hz frequency range. It has been proposed in different sensory systems (for review see Singer, 1999) that oscillatory synchronization between unitary activities could provide a temporal link between those cells. Populations of cells temporally linked together have been called a neuronal assembly (Hebb, 1949). In the olfactory system, relationships between unit activities and oscillatory field potentials have been studied in the insect (Laurent & Davidowitz, 1994; Wehr & Laurent, 1996; Perez-Orive *et al*., 2002): phase locking of unitary activities onto field potential oscillations could play a role in temporal linking of activities for odour-specific neuronal assemblies. In the rabbit, Kashiwadani *et al*. (1999) described synchronized oscillations during odour-evoked spike discharges of neighbouring mitral cells as a possible correlate of temporal binding. Although the results were very interesting at the time, recordings were performed from a single cellular type (mitral/tufted cells), animals were artificially breathing and field potentials were described as exhibiting an oscillatory activity in a single frequency band. Finally, there is little evidence for the temporal relationship between respiratory waves, fast oscillations and unitary discharges across the different layers of the OB. Our study revealed that oscillatory activity is expressed in different frequency bands, at different times during the respiratory cycle, and with a highly differentiated relationship to unitary discharges in different layers of the OB.

Correspondence: Dr Nathalie Buonviso, as above.
E-mail: buonviso@olfac.univ-lyon1.fr

Received 13 December 2002, revised 7 February 2003, accepted 21 February 2003

doi:10.1046/j.1460-9568.2003.02619.x

Materials and methods

Preparation and recording

Experiments were performed on Wistar male rats weighing 200–350 g (IFFA-Credo). Preparation and recordings were carried out in naturally breathing, urethane (1.5 g/kg)-anaesthetized rats. Anaesthesia was maintained by supplemental doses when necessary. All surgical procedures were conducted in strict accordance with the European Communities Council guidelines.

The dorsal region of the OB was exposed. Extracellular single-unit activities and local field potential (LFP) were recorded with 5–8-MΩ glass microelectrodes pulled with a vertical puller (Sutter) and filled with a 0.5-M Na acetate solution saturated with Pontamine Sky Blue (Aldrich, France). Signals were collected from all layers in which unit recordings were possible with our electrodes. We thus recorded in the glomerular layer (GL), the external plexiform layer (EPL), the mitral cell layer (MCL) and the limit between internal plexiform layer and granule cell layer (IPL/GRL). Cells were sampled from the whole antero-posterior axis of the OB and from the whole dorso-ventral axis of the lateral and medial layers. Recording sites were marked with small iontophoretic deposits of Pontamine Sky Blue. Identification of recording sites was performed in serial frozen sections (40 µm thickness) stained with cresyl violet. Along the antero-posterior axis, the total number of sections was split into three parts defining the anterior, median and posterior recording sites, respectively. Following the olfactory ventricle axis, recordings were specified as lateral, ventral or medial. No recording was performed in the dorsal part of the bulb.

The respiratory signal was recorded through a bi-directional airflow sensor placed near the entrance of the nostril. Changes of respiratory airflow were thus measured as a depression during inhalation and a superpressure during exhalation. Electrophysiological recordings were evaluated relative to the transition points between inhalation and exhalation (I/E) which can be automatically detected as 0-crossings of the respiratory signal, corresponding to the point of null pressure variation.

Odours were delivered through a dilution olfactometer (400 mL/min). The recording protocol was the following: 10 s of spontaneous activity, 5 s of odour-evoked activity, 5 s of poststimulus activity. Each sampling included stimulation by at least four odourants: isoamyl acetate, cineole, eugenol and geraniol. We chose to stimulate animals with several odours in order to increase the probability of cell responses. All odours were delivered in front of the animal's nose at a concentration of 18×10^{-2} of the saturated vapor pressure. Each odour presentation was separated from the preceding one by at least 1 min.

Data processing

Bulbar activity was recorded as a broadband signal (0.1 Hz to 5 kHz). All bulbar and respiratory signals were amplified, sampled (10 kHz) and acquired on a PC using the IOTech acquisition system (WaveBook, IOtech Inc., Cleveland, OH).

Unitary activities

Single-unit activity was extracted by band-passing the raw broad band signal from 300 to 3000 Hz (FFT Blackman filter, LabView software). Once spikes were extracted from the signal, each one was time-stamped. These time values were used to calculate firing frequencies and to construct cycle-triggered raster plots. The spontaneous activity of each cell and its activity during the odour-evoked period were first characterized by their mean and maximal frequency. Their type of temporal pattern along the respiratory cycle was characterized and was represented as cycle-triggered raster plots. Based on the pioneer description of Chaput *et al*. (1992), rasters were classified into different types. For the present study, we reduced this classification to four types: (i) unsynchronized patterns, characterized by a uniform distribution of the activity along the respiratory cycle; (ii) excitatory-simple-synchronized patterns, presenting a single increase in firing activity along the respiratory cycle; for these patterns, firing frequency was measured in the single burst; (iii) suppressive-simple-synchronized patterns, presenting a single decrease or stop in firing activity along the respiratory cycle; in these cases, firing frequency was sampled from periods outside the rate decrease; (iv) complex-synchronized patterns exhibiting multiple firing frequency changes along the respiratory cycle; here spike frequency was taken from different bursts. Pattern classification was performed by visual inspection, first independently and then all together by three observers. If at least two of them had chosen the same type for a pattern, they attributed this type to the pattern; otherwise, they decided together the type to which the pattern should be attributed. Because most activity along the respiratory cycle is cyclic, it can be quantified as a mean vector where the angle reflects the mean phase relationship of unit activity with respect to the respiratory cycle. The method has been extensively described elsewhere (Buonviso *et al*., 1992; Chaput *et al*., 1992). Briefly, phase histograms (8° binwidth) of bulbar spike activity relative to respiration were constructed for prestimulation, odour-stimulation and postodour time periods. Mean vectors (angle: 0–360°) describing neural activity and respiratory cycle phase relationships were determined for all cells during each of these time periods, according to the method previously used in auditory (Goldberg & Brown, 1969) or motor (Drew & Doucet, 1991) systems.

LFPs

LFPs were obtained by band-passing the signal recorded via the same electrode as the unit activity at 0.1–200 Hz. Because our aim was to identify and characterize LFP oscillatory activities in time and frequency, we chose a method that preserves both types of information, i.e. a time–frequency representation based on a wavelet transform of the signal. The LFP signal was first down-sampled (208 Hz) and then convoluted by complex Morlet's wavelets $w(t,f_0)$ (Kronland-Martinet *et al*., 1987) which have a Gaussian shape both in the time domain and in the frequency domain around its central frequency f_0 with:

$$w(t,f_0) = A \times \exp\left[t^2/\left(2t_0^2\right)\right] \times \exp(i2f_0t)$$

with

$$f = 1/(2t_0)$$

The wavelet family we use is defined by $f_0/f = 5$, with f_0 ranging from 0 to 100 Hz in 1-Hz steps. The time resolution of wavelet method increases with frequency, whereas the frequency resolution decreases. The time-varying energy $E(t,f_0)$ of the signal in a frequency band around f_0 is defined as the square of the convolution product of the wavelet $w(t,f_0)$ with the signal $s(t)$:

$$E(t,f_0) = [w(t,f_0) \times s(t)]^2$$

In each band, we computed the mean and SD of the time–frequency (TF) in Hz as a function of time and we defined a threshold as the (mean + 5 SD) of the TF energy contained in the prestimulus period (between 0 and 10 s). These thresholds are used to define the starting and final points of a wave as the time instant where the mean TF energy of a band goes above or below the threshold, respectively, in that band. In each identified wave, we searched for the local maximum of the TF energy and then, in the time–frequency representation, we searched for the precise location in time and in frequency of each local maximum found at the previous step. These maxima were represented by their

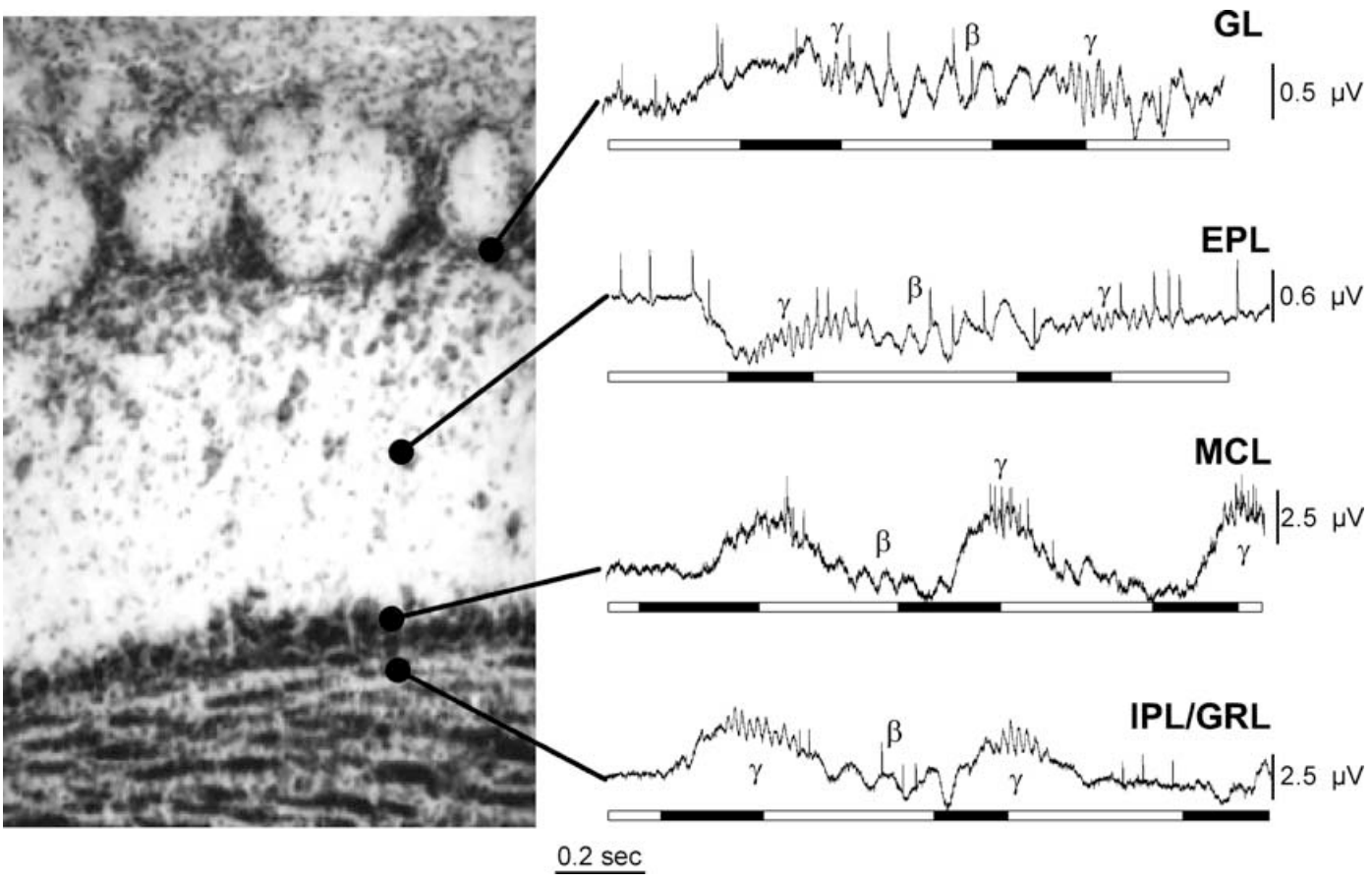

FIG. 1. Left, histological section of the OB, stained with Cresyl Violet, showing GL, EPL, MCL and IPL/GRL. Right, top trace, examples of recordings in the different OB layers during odour stimulation. Bottom trace, representation of respiratory timing: inhalation periods in black, exhalation in white.

phase relative to the respiratory cycle. For that purpose, the respiratory cycle was considered as a sine wave ranging from 0 to 360° where 0 was assigned to the transition point I/E.

Statistics

Spike discharge and oscillations represent different variables, for which a MANOVA with the layer factor was performed to analyse γ- and β-power and spike rates. Univariate tests with, respectively, two-way (layer × repetition) and one-way (layer) ANOVAs were then used to analyse separately measures of spike rates and oscillations features. Multiple comparisons of means were performed with Fisher's test. The normality of the samples and the homogeneity of their variance were controlled with the Lilliefors (Conover, 1971) and the Hartley (Winer, 1962) tests, respectively. Distributions of temporal pattern number obtained for the different cell types were compared with the G-statistic, derived from the likelihood ratio principle, and the χ^2 statistic was used to test the hypothesis of independence. The phase relative to the respiratory cycle was compared between β, γ and spike bursts with the Watson *F*-test, a statistical test specifically designed for circular data such as angles ranging from 0 to 360° (Mardia, 1972; Fisher, 1993).

Results

Responses of 104 cells recorded with their corresponding LFP were analysed in a total of 392 recordings in 33 animals. Among these cells, 28 were sampled in the GL, 20 in the EPL, 47 in the MCL and 9 in the IPL/GRL. The first part of the Results section is devoted to the analysis of LFP oscillations while the second part deals with unitary discharges. Both signals have been processed with respect to the respiratory cycle.

Description of LFP oscillations

Spontaneous LFPs are generally fairly flat. Breathing sometimes causes low amplitude waves $\approx 1.58 \pm 0.27$ Hz. The following descriptions will thus focus on the odour-evoked activity periods. Odour presentation induces oscillatory bursts (Fig. 1) modulated by high amplitude respiratory waves (1.63 ± 0.25 Hz). In order to reliably identify the various oscillatory regimes, LFP signals were analysed using a wavelet transform (see Fig. 2). This analysis determined two peak frequencies of the bursts: one in the γ-frequency range (55.53 ± 7.31 Hz) and one in the β-frequency range (16.51 ± 3.59 Hz). Gamma oscillations usually occur in regular spindles of 70–182 ms duration (mean 117.22 ± 25.05 ms) while β bursts occur in more irregular trains of 2–7 cycles (mean 230 ± 90 ms; Figs 1 and 2A). Table 1 gives mean frequencies of γ and β oscillations in different bulbar layers. One-way ANOVAs showed no significant effect of the layer factor for γ waves ($F_{3,104} = 2.292$, $P = 0.0825$) or for β waves ($F_{3,55} = 2.549$, $P = 0.0651$). No statistical differences could be detected in oscillatory frequencies for the different odourants tested; thus, responses to all stimuli were combined for statistical analyses.

The results of the wavelet transform is illustrated as an energy scalogram which represents the time-varying energy of the signal in each frequency band, leading to a time–frequency representation of the LFP signal. An example of a scalogram is shown in Fig. 2B, which

TABLE 1. Oscillation frequencies in the OB

Layer	γ-frequency range	(*n*)	β-frequency range	(*n*)
GL	53.26 ± 5.46	(34)	17.40 ± 2.68	(10)
EPL	53.72 ± 6.67	(23)	15.18 ± 2.36	(8)
MCL	56.67 ± 6.57	(41)	17.29 ± 4.12	(31)
IPL/GRL	56.14 ± 6.16	(10)	14.27 ± 2.18	(10)

Mean ± SD frequencies of γ and β waves in the different OB layers during odour stimulation. The number indicated in the bracket gives the number of recordings in which respective rhythms could be identified.

highlights several points: (i) high-energy spots of γ activity (≈60 Hz) occur, punctuated by breathing, during the whole presentation of odour; (ii) high-energy spots of β activity (≈12.5 Hz) appear less regularly but also related to breathing; (iii) these two regimes remarkably alternate in time as a function of breathing, and this is well illustrated by the power spectrum extracted for γ and β bands (Fig. 2C). In order to assess such an alternation between the two rhythms, we analysed the respiratory cycle relationship of γ and β bursts. Results presented in Fig. 3 reveal a clear-cut distribution of the two regimes (Watson's *F*-test, $F = 250.88$, $P < 0.001$): while γ oscillations occur almost exclusively around the transition I/E point (mean phase $17.1 \pm 3°$, $n = 57$), β waves occur primarily during a period going from exhalation to the maximal inhalation epoch (mean phase $-139.8 \pm 9°$, $n = 26$). Comparison of circular means (Watson's *F*-tests) did not reveal differences between layers, either for γ- or for β-bursts.

Description of cellular types

Generally, cell types have been established on the basis of the recorded site (GL, EPL, MCL, and IPL/GRL). In the GL, however, visual inspection of data suggested that two different subpopulations of glomerular units could be identified, namely GL1 and GL2 cells, according to their discharge specificity (see below).

In a similar manner to the LFPs, study of unitary discharges focused on odour-evoked activities. Responsiveness of all cell types was tested throughout the bulb. Because χ^2 test revealed no difference in either the antero-posterior axis (anterior/median/posterior, $\chi^2 = 5.7$,

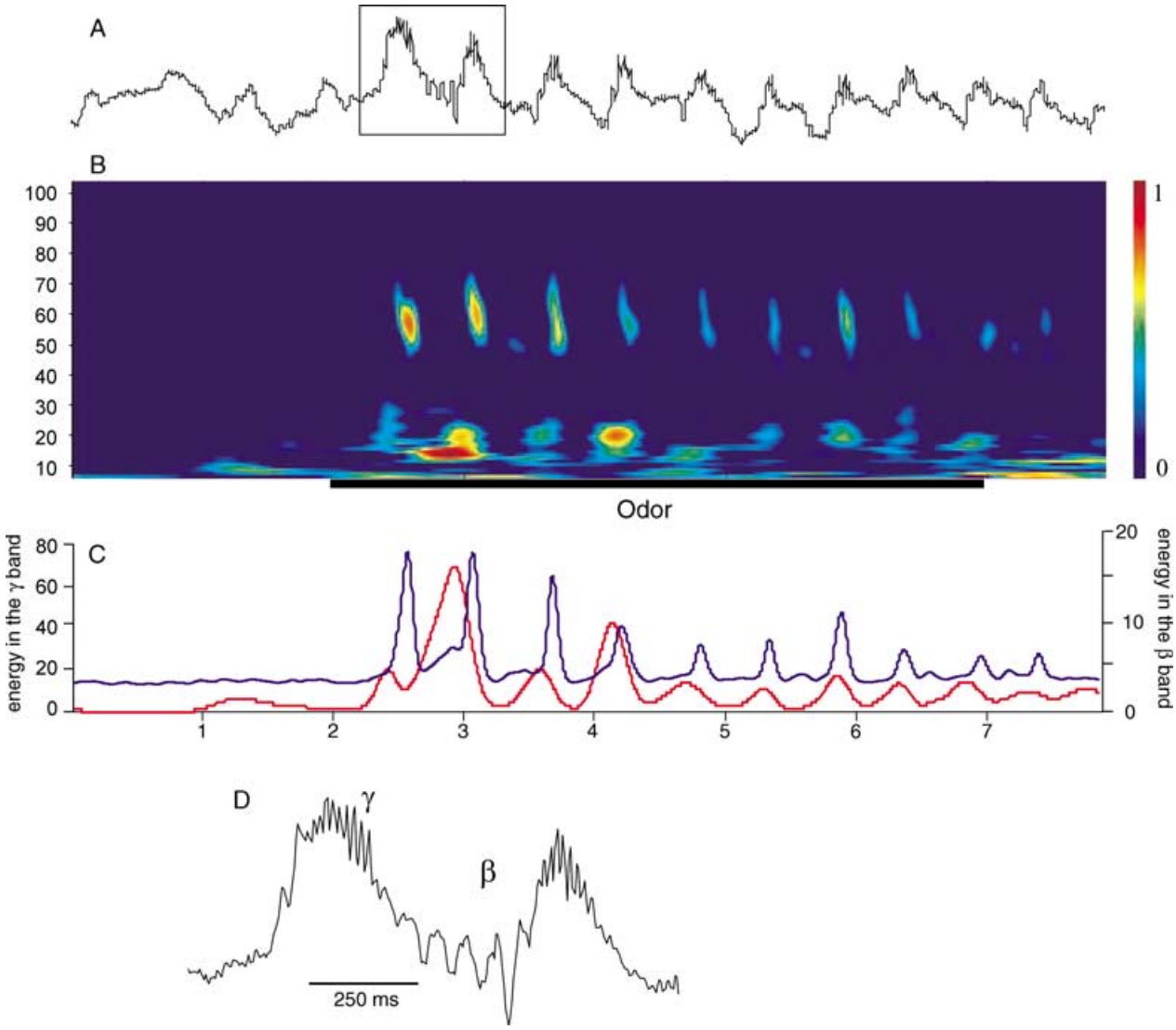

FIG. 2. Time–frequency representation of an LFP signal. (A) Raw signal (0–208 Hz). (B) Corresponding scalogram: *x*-axis, time in s, *y*-axis, frequency from 10 to 100 Hz. Odour-stimulation period is represented by the black bar. The colour scale codes signal power, which is defined relative to the maximal energy of the signal. (C) Energy extracted in the β (10–35 Hz, red) and γ (40–80 Hz, blue) bands. (D) Enlargement of the inset in A.

TABLE 2. Temporal patterns of responses

	GL1	GL2	EPL	MCL	IPL/GRL
Unsynchronised	0	3	7	8	1
Excitatory-synchronised	18*	32*	14*	29*	2
Suppressed-synchronised	0	3	19*	14*	8*
Complex-synchronised	0	4	13*	16*	8*
Responsive cells (%)	94.7	85.7	85.58	75.3	70.4

Table giving the number of cases analysed for each pattern type; *asterisks indicate the cases from which frequencies were calculated. The last line gives the percentage of responding cells relative to the total number of cell stimulated.

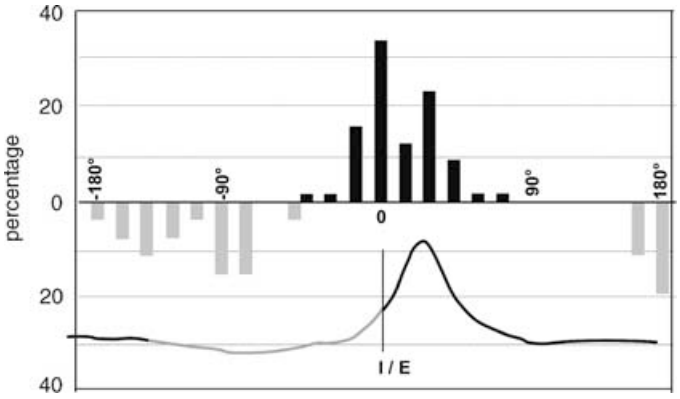

FIG. 3. Phase-locking of β and γ waves relative to respiration. Histograms represent the distribution of the amplitude maxima for β (grey bars) and γ (black bars) oscillations relative to the respiratory cycle. Respiratory cycle is schematically represented in the bottom trace with inhalation in grey and exhalation in black. It is divided into 30° bins (−180° to 180°); 0 represents the I/E transition point.

$P = 0.6$), or following the ventricle axis (median/ventral/lateral, $\chi^2 = 2.21$, $P = 0.33$), data collected from different bulbar areas were combined for statistical analyses.

Temporal patterning and frequency

In order to study temporal relationships between breathing, LFP oscillations and unitary activities, we first classified the diverse cellular types through the temporal patterning of firing over the respiratory cycle and, at the same time, discharge rate was measured in spike bursts. An example of each of the four temporal patterns is presented in Fig. 4A (top). The unsynchronized pattern shows a uniform distribution of spikes along the respiratory cycle; conversely, excitatory-simple-synchronized and suppressive-simple-synchronized patterns reveal an increased and a decreased rate around the I/E point, respectively; the example of complex-synchronized pattern shows an alternation of increased and decreased rates along the respiratory cycle. The χ^2 test revealed that odour quality had no effect on the pattern type ($\chi^2 = 1.96$, $P = 0.99$) and responses to all four odours were pooled. In contrast, a significant difference existed between layers for patterns ($\chi^2 = 246.15$, $P < 0.0001$) and also for discharge rates ($F_{4,108} = 43.73$, $P < 0.0001$). Figure 4 gives the percentages of each temporal pattern (A) and the spike frequencies into bursts (B) for all cell types. Table 2 gives the number of cases analysed where asterisks indicate the pattern types from which frequencies were measured. Figure 4A shows that unsynchronized patterns are unusual. *Post hoc* cell contributions reveal that the number of excitatory-simple-synchronized patterns is higher for GL1 and GL2 cells than for others. It is noteworthy that GL1 cells responded exclusively by excitatory-simple-synchronized patterns. Their behaviour was very stereotyped because they exhibited such a pattern whatever the test odour. As shown in Fig. 4B, spike rate within bursts was very high (183.4 ± 24.8 Hz), leading to a decrease in spike amplitudes towards the end of the bursts (not shown). GL2 cells presented a significantly higher proportion of excitatory-simple-synchronized patterns than of other possible patterns. However, spike frequency within bursts in GL2 cells was lower than for GL1 cells (68.09 ± 8.2 Hz). Responses of unitary activity recorded in the EPL and MCL were more uniformly distributed in the four different temporal patterns and their mean firing frequencies within bursts were not different (49.66 and 55.34 Hz, respectively). IPL/GRL cells most often demonstrated suppressive-simple-synchronized and complex-synchronized patterns. Their patterning was remarkable because they emit either single spikes or 200-Hz short bursts in the β-frequency range (30.7 ± 6.5 Hz). As described by the last line of Table 2, we observed a decrease in responsiveness from GL to IPL/GRL cells. The G-statistic revealed that GL1 cells were significantly more responsive than MCL and IPL/GRL cells ($G^2{}_1 = 4.48$, $P = 0.034$ and $G^2{}_1 = 4.83$, $P = 0.028$, respectively).

Respiratory phase

Second, we compared the relationship between unitary activities and respiration using the method of mean vector analysis. Unlike LFP oscillations, unit respiratory cycle entrainment was significantly different according to the layer (Watson's test, $P < 0.005$), as is easily visible in Fig. 5A raster plots. Figure 5B depicts phase relationships relative to respiration for each cell type. It reveals that GL2 ($n = 10$), EPL ($n = 10$) and MCL ($n = 20$) cells were not significantly different in their respiratory phase locking ($P > 0.3$) because all of them were locked to the transition I/E epoch. Note that the mean phase of γ bursts coincides with the same period (Watson test, $P > 0.1$). An example of MCL activity is presented in the middle raster plot showing an odour-evoked spike burst centred around the I/E point. Conversely, GL1 ($n = 6$) and IPL ($n = 9$) cells appeared very characteristic because the former were phase-locked to the early inhalation period ($P < 0.05$, top raster plot) while the latter discharged preferentially during exhalation ($P < 0.05$). The diagram of mean vectors shows that GL1 cell discharges preceded the γ burst. In contrast, IPL/GRL cells discharged late, during exhalation, as visible in the bottom raster plot and in the mean vector diagram. The Watson test shows no difference between β oscillations and IPL/GRL cell phases.

Discussion

This study showed that odour stimulation induced oscillatory bursts of LFPs in the γ- and the β-frequency ranges in the urethane-anaesthetized rat. Such frequencies have been previously observed in the awake animal (Freeman, 1975; Chapman *et al*., 1998; Chabaud *et al*., 2000). We have shown that, whatever the layer, γ bursts occur around the I/E point while bursts in the β-frequency range are observed during an epoch which starts during exhalation and may last to late inhalation. In previous studies describing such a rhythm, no significance was attached to its relationship with breathing (Chapman *et al*., 1998; Kay & Freeman, 1998; Chabaud *et al*., 2000). In contrast, we describe diverse odour-evoked rhythms coupled to the activity of various cell types of the OB layers. Onoda & Mori (1980) classified OB neurons according to their temporal pattern and depth distribution; however, their results cannot be compared to ours because their recordings were performed with artificial intake of deodourized air. Our study provides evidence that different cellular classes may be established on the basis of the temporal relationships between their spike bursts and LFP oscillations.

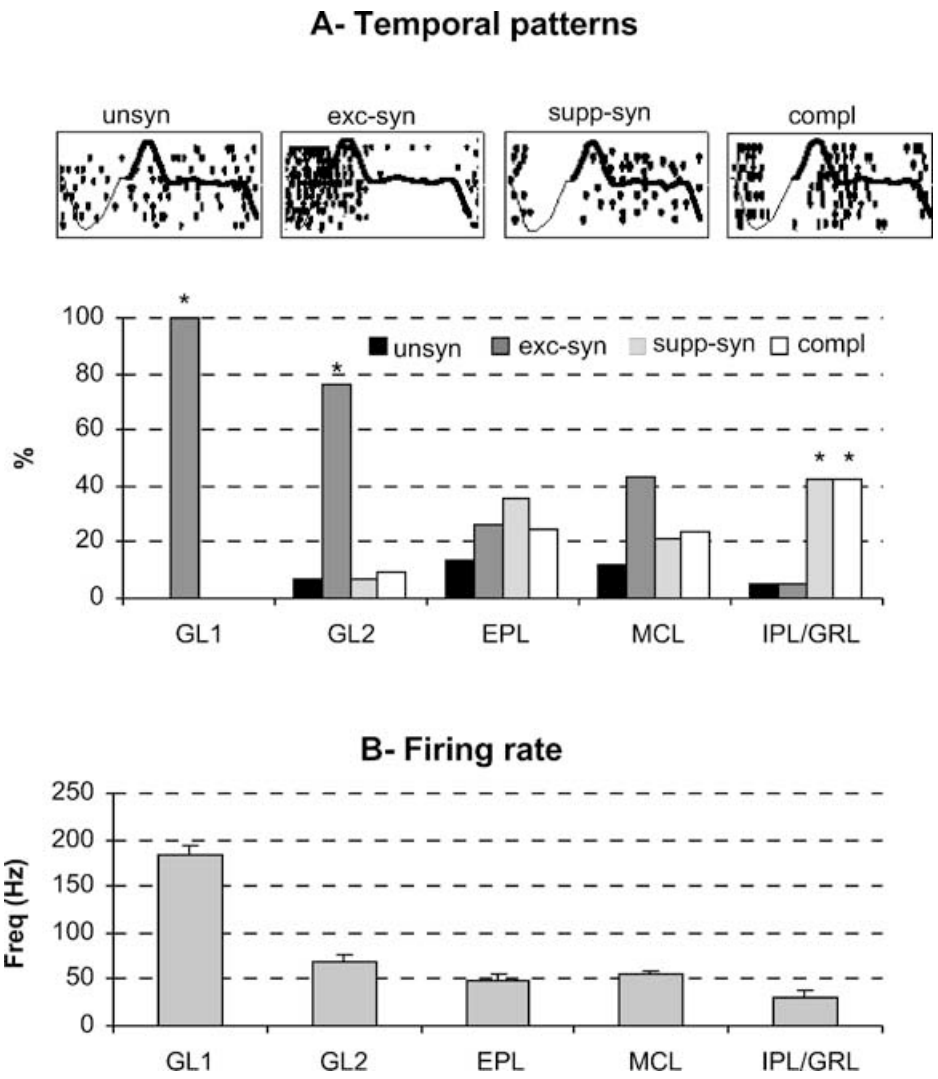

FIG. 4. (A) Temporal patterns. Top, cycle-triggered raster plots showing examples of each type of temporal pattern evoked by odour stimulation. Spikes (dots) are represented as a function of the respiratory cycle. Consecutive respiratory cycles are arranged vertically from bottom to top. The mean respiratory signal is superimposed on each raster plot (Inhalation, thin line; exhalation, thick line). Bottom (histograms), percentages of each pattern evoked by odourant stimulation (all odours pooled) in the five groups of cells. Percentages are calculated with regard to the total number of responses ($^{*}P < 0.05$ vs. the other groups, *post hoc* cell contributions). (B) Mean (+ 1 SD) frequencies of spike burst in each cell group. Frequencies were measured in the cases indicated by asterisks in Table 2. Multiple mean comparisons showed that spike frequencies were significantly higher for GL1 than for the other layers ($P < 0.0001$), significantly higher for GL2 than for EPL and IPL/GRL ($P = 0.0240$ and 0.0003, respectively), and significantly higher for MCL than for IPL/GRL ($P = 0.0085$).

Unitary activities

The main finding of this study is the observation that odour stimulation leads to a succession of rhythms in spike discharges, during the time window of a respiratory cycle, through the depth of the layers, going from a very rapid and early (inhalation) one in glomerular layer cells to a slower and later (transition I/E) one in MCL units, up to a much slower and very late (expiration) one in IPL/GRL neurons.

Glomerular layer

We found here two types of cells, GL1 and GL2. The most typical one, the GL1 type, is characterized by an early (inhalation) high-frequency bursting discharge while temporal patterns and spike frequency of GL2 cells are more variable. We found in the literature two descriptions of cells that could fit with our GL1 type. First, in their intracellular study, Wellis & Scott (1990) reported that odour-evoked responses of periglomerular cells were characterized by very simple bursts of spikes, with a decreasing amplitude and no selectivity. Second, in a recent patch-clamp study, McQuiston & Katz (2001) demonstrated a subpopulation of juxtaglomerular cells exhibiting a low-threshold calcium-dependent spike on the crest of which fast action potentials occur. Our GL1 cells could be those cells which these authors have identified as either external tufted or periglomerular cells. In the same study, McQuiston & Katz (2001) also described a class of neurons with standard activities, without low-threshold spikes, which could be periglomerular, short-axon or external tufted cells. The diversity of responses we observed in GL2 cells could thus represent a diversity of cellular types.

External plexiform layer

This layer offers various types of activities in terms of temporal patterns and discharge rate, according to the depth in the layer. Such diversity can be easily explained by the fact that a number of cell types have been described in this layer, including external, middle and

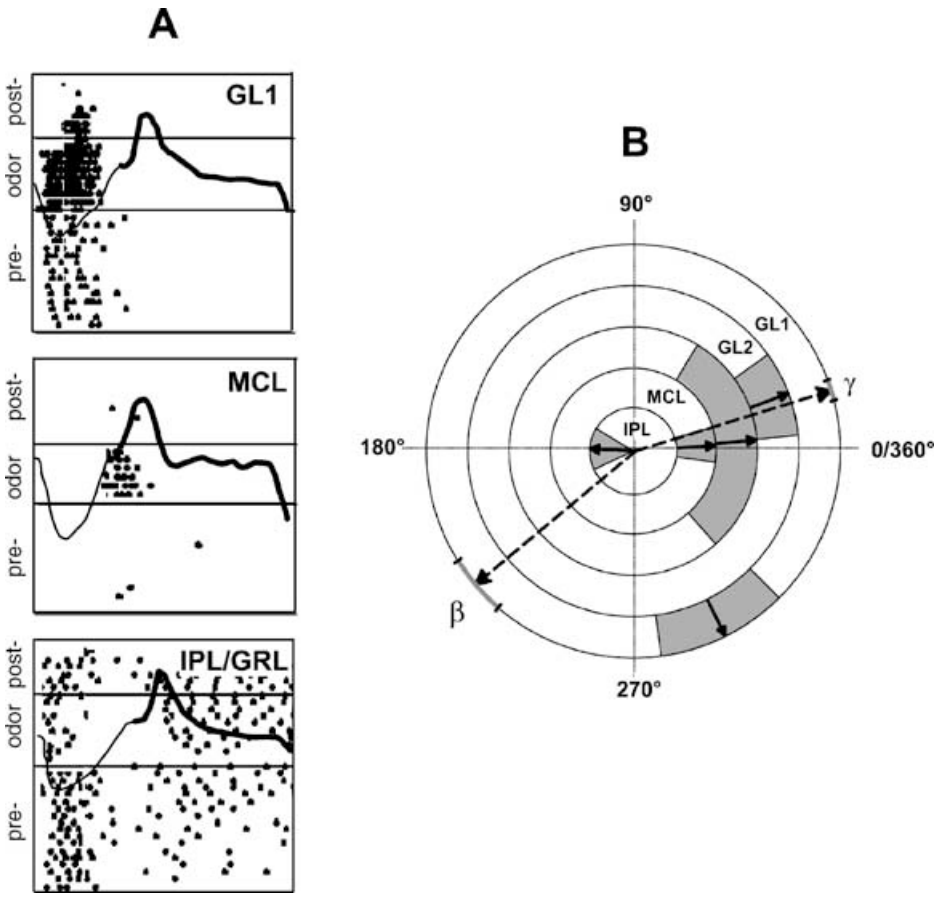

FIG. 5. (A) Examples of cycle-triggered raster plots obtained from three typical activities of GL1, MCL and IPL/GRL cells. Spikes (dots) are represented as a function of the respiratory cycle. Consecutive respiratory cycles are arranged vertically from bottom to top. The mean respiratory signal is superimposed on each raster plot (inhalation, thin line; exhalation, thick line). (B) Mean vector plots of OB unit activities (solid arrows), along with β and γ wave (dotted arrows) mean phase as a function of respiratory cycle. Grey boxes represent 2 SD. The transition I/E point is roughly located around the γ vector.

internal tufted cells, superficial short axon cells and Van Gehuchten cells (Schneider & Macrides, 1978).

Mitral cell layer

Cells recorded in the MCL present the typical features described peviously (Buonviso *et al*., 1992; Chaput *et al*., 1992). Their responses often consist of spike bursts synchronized with the transition I/E period, as was the case for the LFP γ bursts. We showed that spike bursts and γ oscillations are in the same frequency range. This confirms both the empirical study of Eeckman & Freeman (1990) and the observation of Kashiwadani *et al*. (1999) in the rabbit showing a phase locking of mitral/tufted cell discharges to ≈38 Hz LFP oscillations.

Internal plexiform layer

We found that cells located in IPL/GRL present a late (exhalation) and low-frequency discharge. To our knowledge, no report existed before on the activity of such neurons. Cells with somata located in this zone have been described as Cajal cells and horizontal cells by Schneider & Macrides (1978). More recently, a class of interneurons has been observed in this region with the rabies virus (Astic *et al*., 1993): due to their early labelling, they have been interpreted as horizontal cells with axons projecting into glomeruli. Thus, neurons we recorded in the IPL/GRL might be interneurons. This could explain the temporal lag between MCL cell and IPL/GRL cell bursts. Our data do not allow us to infer the contribution of such neurons in LFP β oscillations.

Role of the rhythm sequence: a hypothesis

Figure 6 summarizes the sequence of rhythms we observed in different layers of the bulb and the cell types possibly involved. In the peripheral layer (GL), a subpopulation of cells, activated by almost all odourants, emit spike bursts with high frequency (180 Hz) during inhalation, thus preceding the γ oscillations. These cells could be external tufted cells and/or superficial short axon cells. By studying orthodromic and antidromic response properties of various bulbar cells, Schneider & Scott (1983) showed that these kinds of neurons were very excitable cells and most of them projected their axon toward the granular layer. Because they were very poorly selective and easily excitable with the shortest latency (Schneider & Scott, 1983), these cells could subserve a network-priming function. Moreover, as suggested by McQuiston & Katz (2001), the projection of these bursting neurons to deeper layers may generate (or at least initiate) oscillations in the granular layer.

Next, another population of cells, probably including deeper tufted and mitral cells, is activated. They have ≈50-Hz spike bursts, like the γ waves that occur around the I/E point. This epoch fits with the time of maximal amplitude of the electro-olfactogram (Chaput, 2000) so that it can be suspected to be the time of maximal second-order neuron recruitment. It has been shown that most of mitral/deep tufted cell response pattern consist of spike bursts synchronized around this point (Chaput *et al*., 1992). In addition, mitral cells projecting to a single glomerulus present a high probability to burst synchronously at this

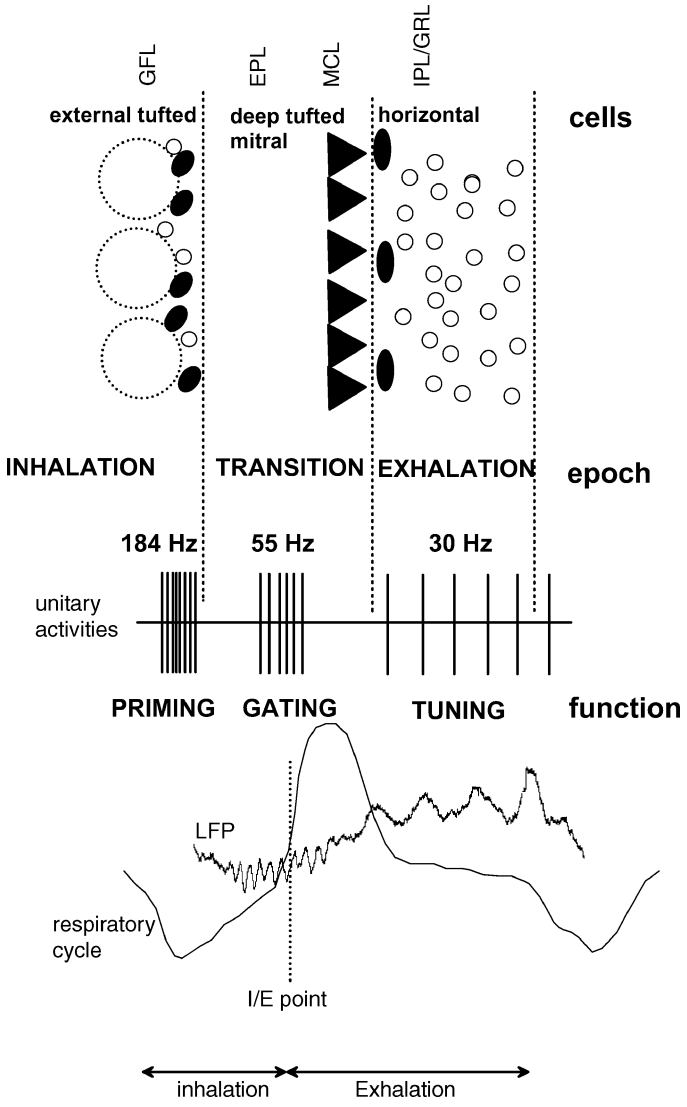

FIG. 6. Schematic representation of rhythm succession in the different OB layers and their hypothesized functions.

time (Buonviso *et al*., 1992). The I/E transition period thus appears as a crucial time window during which cortical structures might sample information. Given that oscillations also exist in the olfactory cortex (Bressler & Freeman, 1980), the simultaneous occurrence of γ rhythms in both structures is suggestive of information transfer if one assumes a mechanism of synchronous transmission, as, e.g. put forward by Abeles (1991). Thus, γ-band oscillations could subserve a kind of gating function for bulbo-cortical transfer of information.

Lastly, in deeper layers, activity of cells discharging with a slower rhythm in the β-frequency range appears during exhalation, much after the γ wave, concomitantly with the β LFP oscillatory activity. We found few cells with such features, probably because we voluntarily rarely lowered the electrode below the MCL and because of the scarcity of these cells. A modelling study of the CA1 region of the hippocampus suggested that β rhythm is much better adapted to synchronization between remote structures (Kopell *et al*., 2000). This hypothesis has been verified experimentally in the awake cat (Roelfsema *et al*., 1997) and in human (Tallon-Baudry *et al*., 2001), showing that β activity is correlated with long-range synchronization of oscillatory activity in distant regions. In the olfactory system, β LFP activity has been shown to be related to odourant input (Chapman *et al*., 1998) but also to centrifugal modulation (Bressler, 1984; Chabaud *et al*., 2000). Particularly, Kay & Freeman (1998) demonstrated a centrifugal β band input from the entorhinal cortex to the OB which is associated with expectation of the learned odour. As suggested by these authors, β rhythm may 'act as a perceptual tuning mechanism in attention or focused arousal.' We would therefore predict that centrifugal fibres originating in the cortex could exert some kind of a tuning function such that representations of expected odours are facilitated if they occur. This could be achieved through interneurons like horizontal cells by re-injecting β-activity into glomeruli during expiration.

This study leads to the conclusion that the time window of a respiratory cycle can be split into three main epochs as a function of LFP and cellular activities among the different OB layers. These different rhythms might serve different functions (as priming, gating and tuning), each one having an optimal efficiency during a particular epoch of the respiratory cycle and quite likely under feed-back control from olfactory cortex, which probably reflects the system's expectancy.

Acknowledgements

The authors thank Michel Vigouroux and Bernard Bertrand for amplifiers and olfactometer conception, Donald A. Wilson for helpful comments on the manuscript, Florette Godinot for help with histology and the anonymous referee for his careful review and very useful suggestions.

Abbreviations

EPL, external plexiform layer; GL, glomerular layer; I/E, inhalation/exhalation; IPL/GRL, internal plexiform layer/granular layer; LFP, local field potential; MCL, mitral cell layer; OB, olfactory bulb; TF, time–frequency.

References

Abeles, M. (1991) *Corticonics – Neural Circuits of the Cerebral Cortex*. Cambridge University Press, Cambridge.

Adrian, E.D. (1950) The electrical activity of the mammalian olfactory bulb. *Electroencephalogr. Clin. Neurophysiol.*, **2**, 377–388.

Astic, L., Saucier, D., Coulon, P., Lafay, F. & Flamand, A. (1993) The CVS strain of rabies virus as transneuronal tracer in the olfactory system of mice. *Brain Res.*, **619**, 146–156.

Bressler, S.L. (1984) Spatial organization of EEGs from olfactory bulb and cortex. *Electroencephalogr. Clin. Neurophysiol.*, **57**, 270–276.

Bressler, S.L. (1987) Relation of olfactory bulb and cortex. II. Model for driving of cortex by bulb. *Brain Res.*, **409**, 294–302.

Bressler, S.L. & Freeman, W.J. (1980) Frequency analysis of olfactory EEG in cat, rabbit and rat. *Electroencephalogr. Clin. Neurophysiol.*, **50**, 19–24.

Buonviso, N., Chaput, M.A. & Berthommier, F. (1992) Temporal pattern analyses in pairs of neighboring mitral cells. *J. Neurophysiol.*, **68**, 417–424.

Chabaud, P., Ravel, N., Wilson, D.A., Mouly, A.M., Vigouroux, M., Farget, V. & Gervais, R. (2000) Exposure to behaviourally relevant odour reveals differential characteristics in rat central olfactory pathways as studied through oscillatory activities. *Chem. Senses*, **25**, 561–573.

Chapman, C.A., Xu, Y., Haykin, S. & Racine, R.J. (1998) Beta-frequency (15–35 Hz) electroencephalogram activities elicited by toluene and electrical stimulation in the behaving rat. *Neuroscience*, **86**, 1307–1319.

Chaput, M.A. (1986) Respiratory-phase-related coding of olfactory information in the olfactory bulb of awake freely-breathing rabbits. *Physiol. Behav.*, **36**, 319–324.

Chaput, M.A. (2000) EOG responses in anesthetized freely breathing rats. *Chem. Senses*, **25**, 695–701.

Chaput, M.A., Buonviso, N. & Berthommier, F. (1992) Temporal patterns in spontaneous and odor-evoked mitral cell discharges recorded in anaesthetized freely breathing animals. *Eur. J. Neurosci.*, **4**, 813–822.

Chaput, M. & Holley, A. (1980) Single unit responses of olfactory bulb neurons to odor presentation in awake rabbits. *J. Physiol. (Paris)*, **76**, 551–558.

Conover, W.J. (1971) *Practical Nonparametric Statistics*. Wiley, New York.

Desmaisons, D., Vincent, J.D. & Lledo, P.M. (1999) Control of action potential timing by intrinsic subthreshold oscillations in olfactory bulb output neurons. *J. Neurosci.*, **19**, 10727–10737.
Drew, T. & Doucet, S. (1991) Application of circular statistics to the study of neuronal discharge during locomotion. *J. Neurosci. Meth.*, **38**, 171–181.
Eeckman, F.H. & Freeman, W.J. (1990) Correlations between unit firing and EEG in the rat olfactory system. *Brain Res.*, **528**, 238–244.
Fisher, N.I. (1993) *Statistical Analysis of Circular Data*. Cambridge University Press, Cambridge.
Freeman, W.J. (1975) *Mass Action in Nervous System*. Academic, New York.
Freeman, W.J. & Schneider, W. (1982) Changes in spatial patterns of rabbit olfactory EEG with conditioning to odors. *Psychophysiology*, **19**, 44–56.
Goldberg, J.M. & Brown, P.B. (1969) Response of binaural neurons of dog superior olivary complex to dichotic tonal stimuli: some physiological mechanisms of sound localization. *J. Neurophysiol.*, **32**, 613–636.
Heale, V.R. & Vanderwolf, C.H. (1994) Dendate gyrus and olfactory bulb responses to olfactory and noxious stimulation in urethane anaesthetized rats. *Brain Res.*, **652**, 235–242.
Hebb, D.O. (1949) *The Organization of Behavior.* Wiley, New York.
Kashiwadani, H., Sasaki, Y.F., Uchida, N. & Mori, K. (1999) Synchronized oscillatory discharges of mitral/tufted cells with different molecular receptive ranges in the rabbit olfactory bulb. *J. Neurophysiol.*, **82**, 1786–1792.
Kay, L.M. & Freeman, W.J. (1998) Bidirectional processing in the olfactory-limbic axis during olfactory behavior. *Behav. Neurosci.*, **112**, 541–553.
Kopell, N., Ermentrout, G.B., Whittington, M.A. & Traub, R.D. (2000) Gamma rhythms and beta rhythms have different synchronization properties. *Proc. Natl Acad. Sci. USA*, **97**, 1867–1872.
Kronland-Martinet, R., Morlet, J. & Grossmann, A. (1987) Analysis of sound patterns through wavelet transforms. *Int. J. Patt. Recogn. Art. Intell.*, **1**, 273–302.
Laurent, G. & Davidowitz, H. (1994) Encoding of olfactory information with oscillating neural assemblies. *Science*, **265**, 1872–1875.
Macrides, F. & Chorover, S.L. (1972) Olfactory bulb units, activity correlated with inhalation cycles and odor quality. *Science*, **175**, 84–87.
Mair, R.G. (1982) Response properties of olfactory bulb neurons. *J. Physiol. (Lond.)*, **326**, 341–359.
Mardia, H.V. (1972) *Statistics of Directional Data*. Academic Press, London.
McQuiston, A.R. & Katz, L.C. (2001) Electrophysiology of interneurons in the glomerular layer of the rat olfactory bulb. *J. Neurophysiol.*, **86**, 1899–1907.
Onoda, N. & Mori, K. (1980) Depth distribution of temporal firing patterns in olfactory bulb related to air-intake cycles. *J. Neurophysiol.*, **44**, 29–39.
Pager, J. (1985) Respiration and olfactory bulb unit activity in the unrestrained rat: statements and reappraisals. *Behav. Brain Res.*, **16**, 81–94.
Perez-Orive, J., Mazor, O., Turner, G.C., Cassenaer, S., Wilson, R.I. & Laurent, G. (2002) Oscillations and sparsening of odor representations in the mushroom body. *Science*, **297**, 359–365.
Rall, W. & Shepherd, G.M. (1968) Theoretical reconstruction of field potentials and dendrodendritic synaptic interactions in olfactory bulb. *J. Neurophysiol.*, **31**, 884–915.
Roelfsema, P.R., Engel, A.K., Konig, P. & Singer, W. (1997) Visuomotor integration is associated with zero time-lag synchronization among cortical areas. *Nature*, **385**, 157–161.
Schneider, S.P. & Macrides, F. (1978) Laminar distributions of interneurons in the main olfactory bulb of the adult hamster. *Brain Res. Bull.*, **3**, 73–82.
Schneider, S.P. & Scott, J.W. (1983) Orthodromic response properties of rat olfactory bulb mitral and tufted cells correlate with their projection patterns. *J. Neurophysiol.*, **50**, 358–378.
Singer, W. (1999) Neuronal synchrony: a versatile code for the definition of relations? *Neuron*, **24**, 49–65.
Tallon-Baudry, C., Bertrand, O. & Fischer, C. (2001) Oscillatory synchrony between human extrastriate areas during visual short-term memory maintenance. *J. Neurosci.*, **21**, RC177(1–5).
Walsh, R.R. (1956) Single spike activity in the olfactory bulb. *Am. J. Physiol.*, **186**, 255–257.
Wehr, M. & Laurent, G. (1996) Odor encoding by temporal sequences of firing in oscillating neural assemblies. *Nature*, **384**, 162–166.
Wellis, D.P. & Scott, J.W. (1990) Intracellular responses of identified rat olfactory bulb interneurons to electrical and odor stimulation. *J. Neurophysiol.*, **64**, 932–947.
Winer, B.J. (1962) *Statistical Principles in Experimental Design*. McGraw-Hill, New York.